Characteristic Analysis of Various Structural Shapes of Superconducting Field Coils

Ji Hyung Kim, SaIl Park, Thanh Dung Le, Kwang Lok Kim, Haigun Lee, Young-Sik Jo, Yong Soo Yoon, and Ho Min Kim

***Abstract*—Superconducting field coils consist of race-track-type double pancake (DP) coil modules fabricated using high-temperature superconducting (HTS) wire with high current density and zero resistance. The structural shape of race-track-type DP coils strongly influences the intensity and the shape of the magnetic flux density in the air-gap, which determines the generator electrical output and the superconducting field coil performance. Hence, the structural shape of a superconducting field coil is very important in designing a large-scale superconducting generator. We analyze the characteristics of a 10-MW-class HTS generator using 3-D finite-element analysis software to investigate the electromagnetic effects due to the structural-shape changes in the superconducting field coil.**

***Index Terms*—High temperature superconducting (HTS) synchronous generator, induced voltage, magnetic flux density, race–track-type double pancake (DP) field coil.**

I. Introduction

MOST field pole superconducting coils in currently developed superconducting rotating machines have been designed and fabricated in a race-track double pancake (DP) coil form. Each coil is wound by high-temperature superconducting (HTS) wire manufactured in tape form with an oblong shape and divided into several DP coil modules to reduce the maximum magnetic flux density, which strongly influences the superconducting field coil performance, and to facilitate field coil maintenance.

Generally, the rotating machine performance is dependent on the magnetic flux density and shape in air-gap or the armature windings. Therefore, the structural-shape design of race-track-type DP field coils is one of the major parameters in designing superconducting rotating machines. It directly and indirectly influences the generator performance by affecting the air-gap linkage flux and magnetic flux density of the field coil, respectively. It also influences the reliability of the superconducting field coil. The structural shape of a field coil for a rotor pole determines the electrical air-gap shape, directly influencing the generator performance and the magnetic field distribution produced by the field coils [1], [2]. Specifically, the magnitude and harmonic contents of the linkage flux can be varied depending on the air-gap shape. Further, the electromagnetic and mechanical characteristics of the field coils are affected by both the size and arrangement of single pancake (SP) coils, which depend on the structural-shape change in the field coils. Therefore, analysis of the characteristic changes in terms of the generator and field coil performance is essential.

This study focuses on the structural-shape design and characteristics analysis of the superconducting field coil of a 10-MW-class HTS synchronous generator already conceptually designed using a 2D analytical design code and 3D finite-element analysis (FEA) at Jeju National University, Korea [7]. First, we designed superconducting field coils with three structural-shape types in accordance with the shape of superconducting field coils designed by researchers for large-scale superconducting rotating machines used worldwide [1]–[7]. Then, we analyzed the electromagnetic characteristics of a 10-MW-class HTS synchronous generator using a commercial 3D FEA to study the electromagnetic effects. We specifically focused on the magnitude and harmonic contents of the induced voltage and the armature linkage flux, in addition to the electromagnetic force in the field coil, which depends on the changes in the field coil structural shape. Finally, we have conducted optimal analyses for generator output voltage in terms of the structural-shape change of the field coil.

II. Shape Design of HTS Race-Track Field Coils

The Introduction section presented that the armature magnetic flux density B_0 is generated by the magnetic flux density of the superconducting field coil and directly affects the linkage flux shape and intensity. Thus, B_0 is the key factor in determining the generator phase induced voltage E_0 in the armature windings which can be expressed as

$$E_0 = \frac{1}{\sqrt{2}} \frac{2\pi N_0}{60} \cdot r_a \cdot B_0 \cdot l \cdot n_0 \cdot q \cdot P \quad (1)$$

where N_0 is the rated revolution, r_a is the mean radius of the armature winding, l is the effective length along the generator axis, n_0 is the number of armature conductor turns in each slot, q is the slot number per phase and per pole, and P is the pole number. B_0 can be changed by the structural shape of the

Manuscript received August 9, 2014; accepted October 30, 2014. Date of publication November 5, 2014; date of current version January 19, 2015. This work was supported by the International Collaborative R&D Program of the Korea Institute of Energy Technology Evaluation and Planning (KETEP) grant funded by the Korea government Ministry of Trade, Industry, and Energy (No. 20118520020020).

J. H. Kim, S. I. Park, T. D. Le, and H. M. Kim are with the Department of Electrical Engineering, Jeju National University, Jeju-si 690-756, Korea (e-mail: hmkim@jejunu.ac.kr).

K. L. Kim and H. G. Lee are with the Department of Materials Science and Engineering, Korea University, Seoul 136-701, Korea, (e-mail: haigunlee@korea.ac.kr).

Y.-S. Jo is with the Korea Electrotechnology Research Institute, Changwon-si 642-120, Korea (e-mail: ysjo@keri.re.kr).

Y. S. Yoon is with the Department of Electrical Engineering, Shin Ansan University, Ansan-si 425-792, Korea (e-mail: ysyoon@sau.ac.kr).

Color versions of one or more of the figures in this paper are available online at http://ieeexplore.ieee.org.

Digital Object Identifier 10.1109/TASC.2014.2367040

race-track DP field coil, which is a critical factor; thus, the field coil structural shape must be considered in the design.

Two main factors influence the design of superconducting field coils. The first factor is the function of the inner radius (r_i), thickness (t_c), and height (h_c) of the field coil. It is mentioned that the generator performance depends on not only the current density but also the superconducting field coil dimensions. When r_i is large, the linkage and harmonic contents of the air-gap flux increases and decrease, respectively. Further, the maximum perpendicular component of the magnetic flux density (B_p), which acts on the field coils and decreases operating current (I_{op}) is increased. As t_c further increases, the harmonic contents of the linkage flux decrease, and the maximum magnetic flux density generated by the superconducting field coils (B_{MAX}) increases. Thus, the armature linkage flux increases, whereas the mechanical rigidity of the superconducting field coil weakens [1], [2].

The other factor concerns the arrangement and the number of DP coil modules. When each DP coil is spread widely over the circumference of the rotor-bobbin block surface, the magnetic flux density distribution in the air gap and armature windings approaches a sinusoidal waveform, which increases the linkage flux. The number of DP coil modules is related to the mechanical robustness. The field coil structure is divided into various DP coil modules to reduce the magnetic flux intensity that acts on and influences the superconducting field coil performance; hence, we can design thinner DP coil modules with lower mechanical stress [8].

Because our study focuses only on the analysis of the characteristics with respect to the shape of the field coil, we designed and analyzed superconducting field coils with three different structural shapes such as rectangular (Models 1–3), pyramidal (Models 4 and 5), and spreadable (Model 6) shapes refer to above two factors. The air-gap size of 71.5 mm, the cross-sectional area of the field coils with specific ampere-turns, and geometric space assigned for each pole were assumed to be constant to obtain comparable analysis results of the electromagnetic effects due to the structural-shape changes under identical design conditions.

In the rectangular type, we designed three rectangular-shaped field coils with different dimensions to verify the variable characteristics of the generator according to the variations in r_i, h_c, and t_c. Then, pyramidal- and spreadable-shaped field coils were designed to analyze the generator characteristics by considering the changes in the air-gap shape and the spreadable arrangement of the DP coils. Fig. 1 shows the cross section of each shape of the superconducting field coils, and Table I lists the coil parameter details. When we designed the field coils, we considered shape factor α and the effective area of the conduction cooling from the bobbin block (a_c), as shown by the dark-red dotted line in Fig. 1. In addition, an operating temperature of 35 K was considered for all analysis models. Shape factor α, which determines whether the magnet is thin or thick, is defined as the ratio of the field coil outer radius (r_o) to the field coil inner radius (r_i). For comparison with each other, it is normalized on the basis of 82.5 mm r_i. As α increases, the superconducting DP coils become thicker, indicating that the mechanical stress increases ($\alpha = 1.2$, 1.8, and 3.6 indicates thin, medium, and thick magnets, respectively) [8]. In addition, as a_c becomes larger, the conduction-cooling capability becomes relatively good. The HTS wire length, which is used to fabricate the field coil, is estimated and differs slightly among the analyzed models because the field coil dimensions vary according to the change in the structural shape. Model 3 has the longest HTS wire owing to its longest r_i.

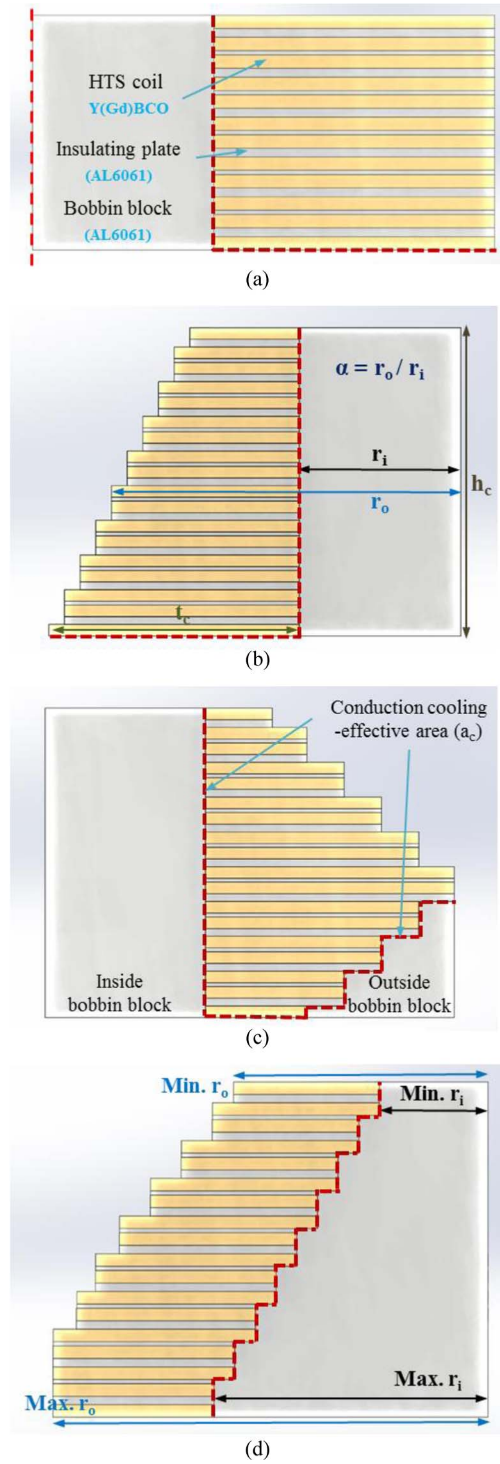

Fig. 1. Cross section of each structural shape for HTS field coils. (a) Rectangular shape of the HTS field coil (Models 1–3). (b) Pyramidal shape I of the HTS field coil (Model 4). (c) Pyramidal shape II of the HTS field coil (Model 5). (d) Spreadable shape of the HTS field coil (Model 6).

TABLE I
PARAMETERS OF THE HTS FIELD COIL WITH DIFFERENT STRUCTURAL SHAPES

Coil parameter [mm]	Structural shape of the HTS field coil: Rectangular Type			Pyramidal type		Spreadable type
	Model 1	Model 2	Model 3	Model 4	Model 5	Model 6
Number of SP coils	12	18	18	18	18	18
Thermal plate number	11	17	17	17	17	17
Turns per pole	9552	9558	9558	9549	9549	9549
HTS wire length [km]	1116	1086	1148	1094	1091	1095
Min. α	2.54	2.03	2.03	1.58	1.42	1.85
Max. α	2.54	2.03	2.03	2.54	2.55	2.18
a_c [m^2]	1.09	1.75	1.18	1.34	1.64	1.48
Min.t_c	127.7	85.3	85.3	48.34	34.4	70.6
Max.t_c	127.7	85.3	85.3	127.5	128	97.9
h_c	106	160	160	160	160	160
Min. r_i	82.5	82.5	124.9	82.5	82.5	52.5
Max. r_i	82.5	82.5	124.9	82.5	82.5	132.5
Min. r_o	210.2	167.8	210.2	138.8	116.9	123.1
Max. r_o	210.2	167.8	210.2	210.2	210.2	210.2

A. Rectangular Shape (Models 1–3)

The rectangular shape, where winding between the DP coils is easy, offers flexibility in the field coil design. It allows various designs of superconducting field coils because space utilization is relatively better; thus, thinner DP coil with smaller α, i.e., higher mechanical stability, can be designed by adjusting the number of SP coils using equal turns in the single pole. However, the cooling efficiency is lower than that of the other shapes because the contact area between the DP coils and bobbin block, which serves as thermal conduction cooling, is relatively small. Model 2 has the largest a_c because it contains two bobbin blocks inside and outside the superconducting field coils.

B. Pyramidal Shape (Models 4 and 5)

To change the air-gap shape, SP coils with different t_c values are stacked in a pyramidal shape. Because α increases toward the bottom SP coils, the bottom mechanical stability is lower than that at the upper SP coils. For Model 5, the cooling capability is enhanced by the surrounding SP coils at the bottom through the outside bobbin block.

C. Spreadable Shape (Model 6)

The spreadable shape has smaller space utilization because the SP coils are spread over the circumference of the bobbin block surface of the rotor. If the geometric space assigned to each pole is not restricted, designing thinner SP coils is possible, which are mechanically excellent because the SP coil arrangement is facilitated by a larger space.

III. CHARACTERISTIC ANALYSIS OF HTS GENERATOR

A. HTS Generator Characteristics

We conducted comparative analysis of each model and simultaneously considered two key parameters that are electromagnetically important factors in designing an HTS generator. The first is the armature linkage flux, which determines the magnitude of the induced voltage. The second is B_{MAX}, which negatively influences the mechanical rigidity and critical current (I_c) of the superconducting field coils. These parameters are very important in the generator stability and performance. Therefore, field coils must be designed and optimized by considering their structural shapes, which can increase the armature linkage flux and decrease B_{MAX}.

TABLE II
ELECTRICAL OUTPUT VOLTAGE CHARACTERISTICS OF THE HTS GENERATOR

Model	Induced voltage (line to line, rms value) Magnitude [V]	VTHD [%]	Linkage flux in the armature (rms value) Magnitude [Wb]	VTHD [%]
1	7912	0.6	364	0.29
2	8714	2.98	401	1
3	10871	1.59	500	0.54
4	7952	3.28	366	1.13
5	8470	2.61	390	0.9
6	8625	3.54	396	1.19

TABLE III
ELECTROMAGNETIC CHARACTERISTICS OF THE HTS GENERATOR

Model	Maximum magnetic flux density: HTS field coil B [T]	B_p [T]	B_l [T]	armature B_r [T]	Electromagnetic force density of HTS field coil Max. magnitude [MN/mm^3]
1	11.9	7.91	11.8	1.95	3100
2	11	7.29	10.9	2.22	2840
3	10.6	8.35	10.5	2.61	2610
4	11.1	7.43	10.8	2	2825
5	11.3	7.46	11.2	2.14	2940
6	10.7	7.53	10.69	2.22	2700

*B, B_p, B_l, and B_r are composite, perpendicular, parallel, and radial component of the magnetic flux density, respectively

The electrical output characteristics, including the line-to-line induced voltage and voltage total harmonic distortion (VTHD) characteristics, were analyzed by comparing Model 1 with Model 2 and Model 2 with Model 3 according to the change in h_c, r_i, and t_c. Thereafter, the electrical output and electro-magnetic characteristics with the magnetic flux distribution and electromagnetic force density of each model were compared to confirm the effects not only of the air-gap shape changes in Models 5–6, but also the spreading arrangement of the DP coil in Model 6.

Tables II and III list the respective comparison results of the electrical output and electromagnetic characteristics of the HTS generator via 3D-transient FEA for steady-state operation of the generator with fully charged operating current of 232 A and rated rotating speed of 10 rpm. In addition, Figs. 2 and 3 show the magnetic field profile from the field coil to the magnetic shield in the radial direction at the center position of the generator and the 3D magnetic field distribution of a 10-MW HTS generator for different field coil shapes, respectively. Significant increment is present on the induced voltage compared with the 6226 V_{RMS} of the based model in [7] because the air-gap size was reduced from 84 to 71.5 mm and the structural shape of the field coils are changed in this study. Moreover, the effect on the reduction in the 2G HTS wire length is significant, indicating savings in the fabrication cost of the field coil for an HTS generator based on 6008-V_{RMS} rated output voltage [7].

1) *Comparison results of Models 1 and 2 (same r_i):* B_{MAX} and the maximum linkage flux of Model 2, which has a higher h_c and smaller t_c and α, are respectively 7.56% smaller and 10% larger than those of Model 1. The field coil shape of Model 2 increases the linkage flux in the armature windings because with equal geometric space assigned to each pole, the distance between the neighbor-

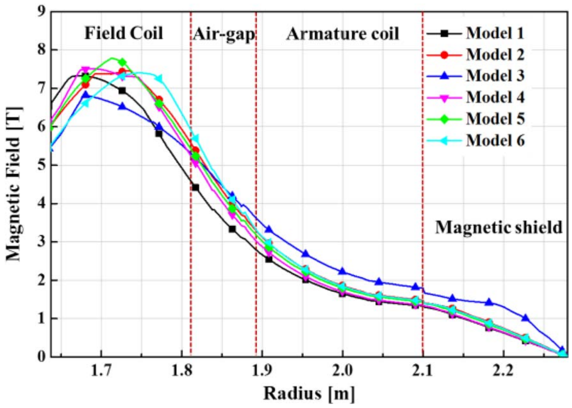

Fig. 2. Magnetic field profile in the radial direction for different coil shapes.

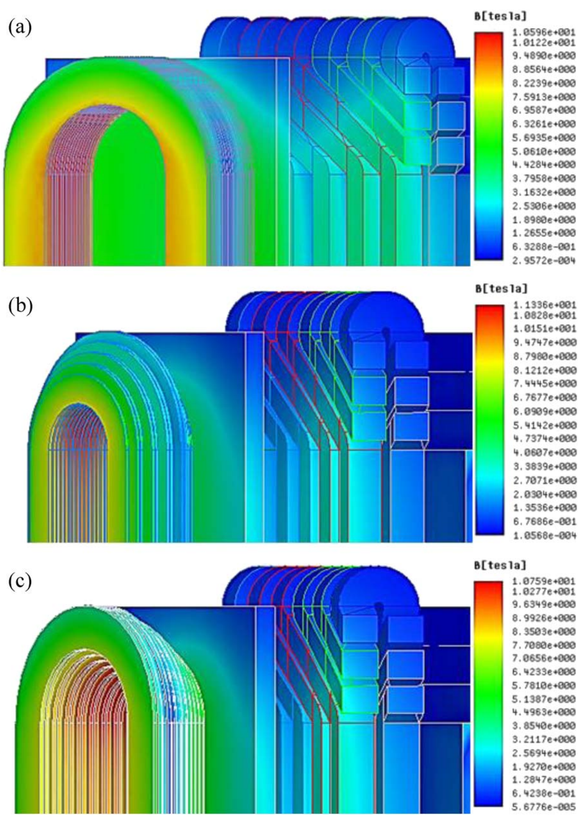

Fig. 3. 3D magnetic field distribution for different field coil shapes. (a) Model 3. (b) Model 5. (c) Model 6.

ing field poles increases with decreasing r_o, which varies with h_c. Thus, the magnetic flux density generated by the field coils cannot pass through the nearby field coils, and the radial component of the magnetic flux density around the armature windings in the air gap increases [3]. Therefore, in the case of equal r_i, designing field coils with larger h_c is advantageous to increase the linkage flux. From the VTHD analysis, the harmonic component in Model 1 with a 127.7-mm t_c is lower than that in Model 2. Accordingly, in terms of the VTHD reduction, designing field coils with larger t_c is better than that with smaller t_c [1].

2) *Comparison results of Models 2 and 3 (same h_c):* B_{MAX} and the maximum linkage flux of Model 3 are respectively 3.63% smaller and 25% larger than those of Model 2. We conclude that as r_i increases, B_{MAX} of the field coil decreases, whereas the armature linkage flux is enhanced. However, as r_i increases, B_p also considerably increases. Hence, r_i should be carefully selected by obtaining the optimal dimensions in the design details to realize stability and performance improvement advantages of the generator [3].

3) *Comparison results between Model 2 and Models 4 and 5 (same r_i):* The rectangular shape of Model 2 is better than the pyramidal shape of Models 4 and 5 from the armature linkage flux perspective. Therefore, the structural shape changes in the field coil have no effect on the air-gap shape change in terms of improvements in the generator power and the VTHD.

4) *Comparison results between Models 4 and 5 and 6:* B_{MAX} of Model 6, designed by spreading DP coil modules, is smaller than that of Models 4 and 5. However, the linkage flux is larger than that of Models 4 and 5. We conclude that the generator power increases via some beneficial effects by the spreading DP coil modules compared with the pyramidal shape of Models 4 and 5. Further, the VTHD of Model 6 is the largest among all models. Unfortunately, we are unable to confirm the spreading effect in terms of harmonic content reduction because Model 6 has unequal minimum r_i compared with the others, as listed in Table II.

The electromagnetic analysis results are as expected. Model 1 has the largest electromagnetic force density because it has a maximum shape factor α of 2.54 compared with the other models with average α of 2.03. Models 3 and 6 present the lowest electromagnetic force density because the maximum α value is distributed by dividing the various DP coil modules. However, for Model 3, the peak electromagnetic force density is generated across the field coils in not only the curve part but also the straight part of the superconducting field coil.

B. Optimization of the HTS Generator Output Voltage

As mentioned earlier, we obtained a significant increment in the induced voltage from the generator characteristic analysis of each model. Hence, the induced voltage must be adjusted to meet the HTS generator design specifications presented in [7].

Two fundamental factors are necessary to optimize the generator output power. The first is the magnetomotive force in the air gap, which generates magnetic flux density B_0 and can be adjusted by controlling the field coil winding turns and I_{op}. The field coil winding turns mean HTS wire length and determination of economic factor of HTS generator. In addition, I_{op} of superconducting field coil is associated with system efficiency and stability.

The second is the amount of air-gap linkage flux that can be adjusted by adjusting the armature conductor turns in each slot n_0, which affect the efficiency, voltage regulation, and synchronous reactance. To reduce the fabrication costs of superconducting field coils and to design a highly reliable HTS generator with efficiency of above 97%, we performed an optimal analysis of the generator output voltage by considering the abovementioned three methods of controlling the winding turns and I_{op} of the rotor field coil and adjusting n_0, as indicated in (1).

TABLE IV
ANALYSIS CONDITIONS TO OPTIMIZE HTS GENERATOR INDUCED VOLTAGE

Model	Field coil winding turns; HTS wire length [km]	Operating Current; Critical current [A]; I_{op}/I_c	Series armature windings per phase; per slot
1	6840; 818	183; 255; 0.72	288; 6
2	7344; 823	166; 288; 0.59	240; 5
3	5058; 623	133; 313; 0.44	192: 4
4	8154; 928	182; 268; 0.69	288; 6
5	7403; 841	171; 278; 0.6	240; 5
6	7027; 811	168; 284; 0.62	240; 5

TABLE V
ANALYSIS RESULTS FOR OPTIMIZATION OF GENERATOR INDUCED VOLTAGE

Model	Field coil winding turns			Operating current		Series armature windings per phase	
	$B_{MAX.}$ [T]	THD [%]	V_{RMS} [V]	$B_{MAX.}$ [T]	V_{RMS} [V]	E_{FF} [%]	V_{RMS} [V]
1	9.18	0.83	6230	9.36	6243	0.83	6399
2	8.95	4.48	6267	7.89	6237	1.25	6097
3	6.43	3.44	6252	6.08	6245	1.68	6412
4	10	3.06	6235	8.65	6240	0.83	6437
5	9.58	2.58	6235	8.35	6245	1.25	5955
6	8.21	3.61	6231	7.79	6248	1.25	6068

*E_{FF}, V_{RMS}, and $B_{MAX.}$ are efficiency increment, line-to-line induced voltage, and maximum magnetic flux density, respectively.

The analysis conditions and optimization results of the generator induced voltage are listed in Tables IV and V, respectively. In the first method, the field coil structural shape was redesigned and analyzed to re-estimate the winding turns of the field coil to generate a 6226-$\mathrm{V_{RMS}}$ induced voltage of the based model presented in [7]. From the re-analyzed results, the VTHD for each model were recalculated, as listed in Table V. From the re-estimation and re-design, we found that HTS wire length savings of from 15.2% (Model 4) to 45.7% (Model 3) can be achieved compared with the values listed in Table I by controlling the field coil winding turns.

In the second method, B_{MAX} was proportionally decreased by setting I_{op}. The proportional reduction in B_{MAX} for each analyzed model was computed in the range from 21.3% (Model 1) to 42.7% (Model 3) based on the previous optimized generator induced voltage. Further, I_c based on 40 K was re-estimated to determine the stability margin of superconducting field coil. I_c and operating current margin (I_{op}/I_c) are listed in Tables IV. Therefore, we can conclude that the I_{op} values are suitable for stable field coil operation.

Finally, the optimization results using the third method show that the generator induced voltage of Models 1–6 ranged from 5955 to 6437 $\mathrm{V_{RMS}}$. The induced voltage for each model was optimized by considering the voltage drop in each phase to meet the rated output voltage, which was varied by the armature turns. Therefore, the generator efficiency in each model improved by as much as 0.83%–1.68% compared to the 96.33% efficiency of the based model. This improvement was due to the copper loss reduction when the armature coil resistance was reduced by adjusting n_0 as shown in Table IV.

As a summary, although we applied only one method in optimal simulation to highlight the effects of the above-described methods, we recommend that pertinent combination of the three methods is essential to precisely adjust the generator output voltage. The characteristics listed in Table V can be further improved by optimal design of the flux damper thickness [9].

More parameter and characteristic variations of the HTS generator that are not considered in this study should be examined, such as voltage regulation. In particular, by controlling the field coil turns, we can expect that more characteristic changes are possible due to the changes in the structural shape, i.e., the dimensions and arrangement of field coil can be changed by reducing the coil winding turns. In addition, mechanical and thermal analyses in terms of the structural shape must be conducted, including mechanical and thermal stresses and temperature distribution, for large-scale HTS generator rated 10 MW and above. Accordingly, adopting a definite field coil shape in this research is premature. More detailed studies need to be conducted.

IV. CONCLUSION

Analytical design and simulations of a 10-MW-class HTS generator according to the structural-shape changes of the superconducting field coil have been performed using 3D FEA.

From each comparative analysis result, we confirm the effects on the HTS generator and field coil performance through function of r_i, t_c, and h_c and determine the effects of the air-gap shape change and the spreading DP coil arrangement. All comparison analyses in this study must be understood to focus only on determining the several effects of the changing structural shape of the superconducting field coil, i.e., this is definitely not the optimal design. Therefore, we recommend fundamental guidelines for designing the structural shape of superconducting field coils from the perspective of electromagnetic performance.

From our optimal analysis results on the generator induced voltage, we conclude that Model 3, which generates the largest induced voltage and lowest magnetic flux density in the superconducting field coil, is suitable for economy, efficiency, and reliability from the HTS generator system perspective.

REFERENCES

[1] R. Shafaie and M. Kalantar, "Design of a 10-MW-class wind turbine HTS synchronous generator with optimized field winding," *IEEE Trans. Appl. Supercond.*, vol. 23, no. 4, Aug. 2013, Art. ID. 5202307.
[2] J. H. Kim *et al.*, "Conceptual design of a field coil for 5 MW HTS synchronous machine," *J. Supercond. Novel Magn.*, vol. 26, no. 4, pp. 1247–1251, Apr. 2013.
[3] J. J. Lee, Y. S. Jo, J. P. Hong, and Y. K. Kwon, "Design of field coil for 100-hp-class HTS motor considering operating current," *IEEE Trans. Appl. Supercond.*, vol. 13, no. 2, pp. 2214–2216, Jun. 2003.
[4] S. Fukui *et al.*, "Numerical study of optimization design of high temperature superconducting field winding in 20 MW synchronous motor for ship propulsion," *IEEE Trans. Appl. Supercond.*, vol. 22, no. 3, Jun. 2012, Art. ID. 5200504.
[5] P. Elhaminia, J. Yaghoobi, M. Yazdanian, M. R. Zolghadri, and M. Ferdowsi, "Comparing different rotor structures in superconducting synchronous motors," in *Proc. IEMDC*, Chicago, IL, USA, 2013, pp. 1053–1057.
[6] J. H. Kim and H. M. Kim, "Electromagnetic design of 10-MW-class superconducting wind turbine using 2G HTS wire," *Progr. Supercond. Cryogenics*, vol. 15, no. 3, pp. 29–34, Sep. 2013.
[7] J. H. Kim, S. I. Park, T. D. Le, and H. M. Kim, "3D electromagnetic design and electrical characteristic analysis of a 10-MW-class high-temperature superconducting synchronous generator for wind power," *Progr. Supercond. Cryogenics*, vol. 16, no. 2, pp. 47–53, Jun. 2014.
[8] Y. Iwasa, *Case Studies in Superconducting Magnets: Design and Operational Issues*, 2nd ed. New York, NY, USA: Springer-Verlag, 2009, pp. 102–105.
[9] H. C. Jo *et al.*, "Numerical analysis and design of damper layer for MW-Class HTS synchronous wind turbine," *IEEE Trans. Appl. Supercond.*, vol. 24, no. 3, Jun. 2014, Art. ID. 5200905.